https://communications.science.ankara.edu.tr

Commun.Fac.Sci.Univ.Ank.Ser. C Biology
Volume 29, Number 2, Pages 23-39 (2020)
ISSN 1303-6025 E-ISSN 2651-3749
https://dergipark.org.tr/en/pub/communb/issue/58140/824616

Received by the Editors: November 11, 2020; Accepted: December 08, 2020

SYNTHESIS AND CHARACTERIZATION OF MCM-41 AND METAL-SUPPORTED MCM-41 MATERIALS USING DIFFERENT METHODS

ÜMRAN GEDİKLİ, ZARİFE MISIRLIOĞLU, PINAR ACAR BOZKURT and MUAMMER CANEL

Department of Chemistry, Ankara University, 06100 Ankara, TURKEY

ABSTRACT. One of the known groups of mesoporous materials is MCM-41 that has been applied as a catalyst for various chemical reactions. MCM-41 was synthesized via hydrothermal and sonochemical synthesis methods using cetyltrimethylammonium bromide (CTAB) as a surfactant, sodium silicate, tetraethylorthosilicate (TEOS) as silica source. The obtained results showed that MCM-41 synthesized by the sonochemical method had higher specific surface area and pore volume than those synthesized by the hydrothermal method. Also, the effects of silica sources on the distribution of products were studied, and sodium silicate was found to be more suitable for the synthesis of MCM-41. Based on the determined optimum conditions, MCM-41 supported Al, Co, and Fe having different ratios of metal (Metal/Si: ratio 0.05, 0.1, and 0.2) was synthesized. It was observed that metal dispersion on MCM-41 was homogenous for all samples and its particle sizes were between 10 nm to 30 nm. Synthesized mesoporous materials were characterized by X-ray diffraction (XRD), scanning electron microscopy (SEM), energy dispersion spectroscopy (EDS), and Brunauer Emmett Teller (BET) surface area methods.

1. INTRODUCTION

After discovering ordered mesoporous materials, the research on the synthesis, characterization, and application of these materials has been accelerated because of their potential use as catalysts, molecular sieves, and hosts for inclusion compounds. The synthesis of these materials is usually done in the presence of surfactant-type organic templates around which the inorganic framework forms [1-2]. One of the family members, MCM-41, which has a large surface area, controllable adsorption properties, and hydrothermal stability, was first synthesized by Mobil Research and

Keyword and phrases. MCM-41, mesoporous materials, hydrothermal method, sonochemical method, synthesis, characterization

umrangedikli@gmail.com; misirli@science.ankara.edu.t; pacar@ankara.edu.tr-Corresponding author; canel@science.ankara.edu.tr
0000-0002-7071-5808; 0000-0002-0195-9606; 0000-0001-8743-9734; 0000-0003-1104-0756

Development Corporation in 1992. There is a growing interest in the material as it can potentially be used as a catalyst, support, and host lattice for advanced secondary organic structures such as conducting filaments [3-4].

There are many methods and many molar compositions of mixture for the synthesis of MCM-41 [5-11]. Source of silica, surfactant, and water as the solvent are three essential components of the mixture used in the synthesis of MCM-41. Generally, cetyltrimethylammonium bromide is used as a surfactant in the synthesis of MCM-41. The template is crucial for the control of the frameworks since it acts as a structure-directing agent. The pores' size can be enlarged or contracted by changing the chain length of the surfactants that are usually used as a template in the composition of the synthesis [1].

Most of the work on mesoporous materials MCM-41 has been synthesized by the direct hydrothermal method in a strong base medium at room temperature. However, there are some defects, such as longer-inducing time and crystal-transforming phenomenon in this method [12-14]. Therefore, the sonochemical method was used as well as the hydrothermal method in this work. The sonochemical method influences the synthesis reaction to proceed with efficiency within a short time and favors metals' good dispersion. The method has been used in different chemical reactions and materials synthesis since sonochemical effects are beneficial to preparing and modifying materials [15].

As a result of the disordered wall structure, MCM-41's acidity was low, close to the levels observed for the zeolites. In an attempt to increase the level of acidity, ion exchange capacity, and the mesoporous silica molecular sieves' catalytic activity, different metal elements are supported in the silica framework of MCM-41. The incorporation of different elements within the silica framework of MCM-41 has been implemented to increase the acidity, ion exchange capacity, and specific catalytic activity of the mesoporous silica molecular sieves. Therefore, synthesizing mesoporous materials by incorporating metal is a significant issue for improving catalytic applications [16-20].

The synthesis of MCM-41 materials by direct hydrothermal synthesis method and sonochemical synthesis method was given briefly in our previous study [21]. In the context of this study, the detail about the synthesis of mesoporous nano-structured MCM-41 materials was explained, and optimum conditions were determined. It was seen that both methods were successful in obtaining the materials with stable crystalline pore structures. Furthermore, to investigate the silica source's effect on the distribution of synthesized MCM-41 materials, sodium silicate and

tetraethylorthosilicate (TEOS) were used as a silica source. Investigation of BET results showed that MCM-41 materials synthesized by the sonochemical method using sodium silicate as a silica source had higher specific surface area and pore volume values. After obtaining the optimum conditions, for catalysts having different metal ratios (Metal/Si: ratio 0.05, 0.1, and 0.2) in its structure, the sonochemical method was used for Al-MCM-41, Co-MCM-41, and Fe-MCM-41. Characterization studies (XRD, SEM, EDS, BET) were performed to determine the structural and physical properties of synthesized catalysts.

2. Materials and methods

2.1. Synthesis of MCM-41 with different silica sources by the hydrothermal synthesis method

To investigate the differences in their effects on the structure of MCM-41, two silica sources were used in the analysis. Firstly, sodium silicate was used as a silica source in the synthesis of MCM-41. 11.3 mL sodium silicate was added to the solution of CTAB (13.2 g CTAB in 70 mL of H_2O). After stirring for 2 hours at room temperature, the resulting gel was transferred into a Teflon-lined stainless steel autoclave and heated in the drying oven for four days at 120°C. The precipitate was filtered, washed thoroughly with distilled water, and dried at ambient temperature. In order to investigate the effect of different calcination temperatures on the structure of MCM-41, the synthesized materials were calcined at 450°C, 550°C, and 650°C for six h. 550°C was chosen as the calcination temperature in the analyses performed as the best results were observed at this temperature.

Second, TEOS was used as a silica source in the synthesis of MCM-41. Accordingly, 2.2g CTAB was dissolved in 52 mL of distilled water and homogenized by magnetic stirring in 1.5 hours. 24 mL NH_3 was added to this solution and stirred for about 30 min at ambient temperature. Following that, 10 mL TEOS was slowly added to the surfactant solution. The reaction mixture was then transferred into a Teflon-lined stainless steel autoclave and heated at 120°C for four days. The solid was filtered, washed, dried at ambient temperature, and finally calcined at 550°C for six h.

2.2. Synthesis of MCM-41 with different silica sources by sonochemical synthesis method

In order to investigate whether using a different synthesis method affects the results, MCM-41 was synthesized using the sonochemical method using sodium silica and TEOS as silica sources. This method was carried out in a Sonics VCX 750 ultrasonic

device with an ultrasound power of 750 W and 20 kHz of frequency. The device was also equipped with a timer and a temperature controller.

The molar composition used in the sonochemical method was the same as described in the hydrothermal method. Silica sources were added to the solution of CTAB. The mixture was stirred for 15 min using one-step sonication and then placed into a Teflon-lined stainless steel autoclave and heated at 120°C for four days. The resulting product was filtered, washed, and dried at an ambient temperature and, finally, calcined at 550°C for six h. The MCM-41 samples obtained under different synthesis methods and silica sources are presented in Table 1.

TABLE 1. Synthesis parameters of MCM-41 samples.

Sample	Method	Silica source
H-1	Hydrothermal	Sodium silicate
H-2	Hydrothermal	TEOS
S-1	Sonochemical	Sodium silicate
S-2	Sonochemical	TEOS

2.3. Synthesis of metal-supported MCM-41

MCM-41 supported by various metals (aluminum, cobalt, iron) in different metal/Si ratios were synthesized using the sonochemical synthesis methods (see Table 2). Aluminum nitrate nonahydrate ($Al(NO_3)_3.9H_2O$), cobalt nitrate hexahydrate ($Co(NO_3)_2.9H_2O$), and iron nitrate nonahydrate ($Fe(NO_3)_3.9H_2O$) were used as Al, Co, Fe sources, respectively. As a first step, the sodium silicate was added to the surfactant solution adopting the method described in Section 2.2. The different amounts of nitrate solutions calculated for the respective metal/Si ratios were added and stirred for 15 min using one-step sonication. The obtained gel was transferred to the autoclave and heated at 120°C for four days. It was filtered, washed with distilled water, and dried at ambient temperature. Finally, the synthesized material was calcined at 550°C for six h.

TABLE 2. Synthesis parameters of metal-supported MCM-41 samples.

Sample	Metal	Molar ratios of metal/ Si
Al-1		0.2
Al-2	aluminum	0.1
Al-3		0.05
Co-1		0.2
Co-2	Cobalt	0.1
Co-3		0.05
Fe-1		0.2
Fe-2	Iron	0.1
Fe-3		0.05

2.4. Characterization

The samples were characterized by X-ray diffraction (XRD), scanning electron microscopy (SEM), energy dispersive X-Ray spectroscopy (EDS), and Braunauer-Emmett-Teller (BET) surface area.

The XRD patterns of the catalysts were recorded by a Rigaku D/MAX 2200 diffractometer with CuKα radiation. The accelerating voltage and applied currents were 40 kV and 30 mA, respectively. The MCM-41 samples were scanned within the range of 2θ= 1-10° while the metal-supported MCM-41 samples were scanned within the range of 2θ= 10-90° with steps of 0.15° (2θ)/min.

The BET analysis was carried out on a Quantochrome-Nova 2200e to achieve the specific surface areas of the supports and catalysts. Each sample was degassed at 110°C for 18 h before the N_2 physisorption.

The synthesized materials' morphology was determined using a Jeol-JSM-6400 Scanning Electron Microscope (SEM) with an accelerating voltage of 20 kV. The materials were coated with gold for the analysis of the sample. The Jeol-JSM-6400 apparatus determined the bulk compositions of the metal-supported MCM-41 materials.

3. Results and Discussion

3.1. Determination of optimum conditions for synthesis mesoporous MCM-41 materials

Calcination temperature plays an essential role in the structure of mesoporous molecular sieve. Thus, different calcination temperatures in the synthesis of MCM-41 were investigated to improve the crystal structure and increase the surface area and porosity. Three different temperatures were used on the H-1 sample for six h and XRD results of all samples shown in Figure1. Two prominent diffraction peaks (100, 110) with weak intensity were seen in the sample XRD pattern on 450°C calcination temperature in Figure 1a. When the temperature reached 550°C, the intensity of the (100) diffraction peak became more substantial, and the (110) and (200) diffraction peaks were also noticeable. At 650°C, the (100) diffraction peak is apparent, and the (110) and (200) diffraction peaks are relatively weak. It is shown that calcination temperature was an important factor for the crystal structure of MCM-41. If the

temperature were too high, the pore would collapse by sintering, and its regularity decreased.

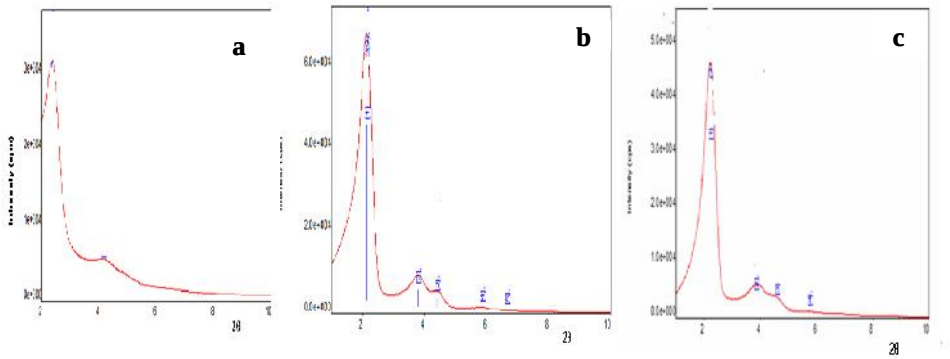

FIGURE 1. X-ray powder diffraction patterns of sample H-1 for different calcination temperatures (a) 450°C, (b) 550°C, (c) 650°C.

The BET surface area and pore volume of the sample on different calcination temperatures were displayed in Table 3. When the calcination temperature was 550°C, the BET surface area and pore volume were maximum. The reason may be that when MCM-41 calcined at 450°C, it did not wholly crystallize, and the pore structure formed only partially. If calcination were performed at 650°C, its pore structure would be destroyed, and the BET surface area was less than that of 550°C.

TABLE 3. BET surface area values and pore volume of H-1 sample for different calcination temperatures.

Calcination temperature (^{0}C)	**BET surface area (m^2/g)**	**Pore volume (cc/g)**
450^{0}C	476	0.498
550^{0}C	959	0.805
650^{0}C	728	0.613

Consequently, a suitable calcination procedure at 550°C for six h was used to prepare all materials. The results were found in agreement with literature values for the influence of calcination temperature on synthesized mesoporous MCM-41 materials [22-24].

The reflections obtained in the low angle region are characteristic of the well-ordered MCM-41 structure with hexagonal. The XRD pattern of H-1, S-1, H-2, and S-2 was

shown in Figure 2. The XRD pattern of the sample H-1 and S-1 exhibited a very sharp diffraction peak corresponding to the (100) plane and three peaks with lower intensities at (110), (200), and (210) planes [25-30]. The XRD pattern of the sample H-2 and S-2 exhibited lower diffraction peaks correspond to the (100) and (110) planes but did not show any peaks corresponding to (200) and (210) planes. These XRD results indicated that MCM-41 catalysts in the hexagonal structure were synthesized with both methods. When the effect of different silica sources on the material characteristics was investigated, it was determined that the crystal structure of material produced by TEOS was worse than the material synthesized with sodium silicate. Also, it was observed expansion on the primary peak and a decrease in intensity of this peak.

Reflection angles, corresponding d-spacing values, and calculated lattice parameter a_0 value for H-1, S-1, H-2, and S-2 samples were determined by X-ray diffraction analyses, and the results were summarized together with BET analyses in Table 4. From the d value obtained from the XRD pattern, lattice parameter a_0 was calculated by the formula given below.

$$a_0 = 2.\frac{d_{100}}{\sqrt{3}}$$

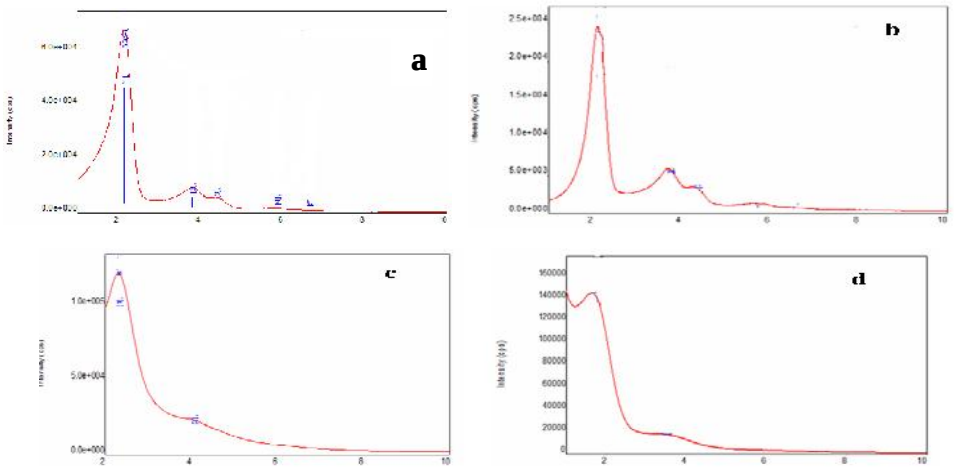

FIGURE 2. X-ray powder diffraction patterns of sample (a) H-1, (b) S-1, (c) H-2, (d) S-2.

As seen from Table 4, the sonochemical method has high values in lattice parameter ao compared with the hydrothermal method, indicating better order material in the

sonochemical method. When the synthesized samples' surface properties were examined, it was observed that high surface area MCM-41 materials with pore sizes in the mesopore range. As can also be understood from the pore volume and the surface area, if the components of MCM-41 are stirred without a sonicator, partial removal of the template from the pores of MCM-41 will be obtained. Using the sonochemical method for synthesis of MCM-41, an increase of surface area and pore volume has been obtained.

TABLE 4. Physical properties of sample H-1, S-1, H-2, and S-2.

Sample	**d-value (nm)**		**2theta (deg)**	**a_0**	**BETsurface area (m^2/g)**	**Pore volume (cc/g)**
H-1	d_{100}	3.945	2.2377	4.555	959	0.805
	d_{110}	2.295	3.847			
	d_{200}	1.931	4.572			
	d_{210}	1.139	5.734			
S-1	d_{100}	4.115	2.1449	4.752	1299	1.078
	d_{110}	2.363	3.736			
	d_{200}	2.026	4.359			
	d_{210}	1.545	5.716			
H-2	d_{100}	2.334	3.782	2.695	345	0.176
	d_{110}	4.067	2.171			
S-2	d_{100}	5.356	1.648	6.184	606	0.407
	d_{110}	2.559	3.450			

The morphology of the synthesized samples was checked by SEM and shown in Figure 3. SEM results showed that each spherical aggregate was composed of several individual small nanoparticles with uniform diameters of about 60 nm. Fig. 3 (a-b) demonstrated that the spherical particles were extensively agglomerated. The sponge-like appearance of the MCM-41 particles was seen in Fig. 3 (c-d). It was concluded that the used silica source affected the morphology of the synthesized MCM-41 material.

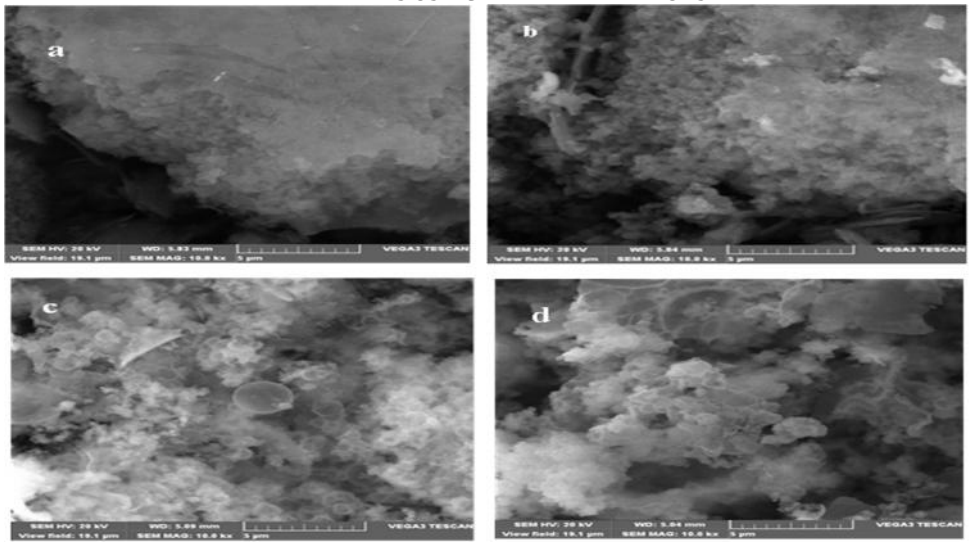

FIGURE 3. Scanning electron micrographs for sample (a) H-1, (b) S-1, (c) H-2, (d) S-2.

According to the results obtained with characterization studies, we can conclude that the sonochemical method using sodium silicate as a silica source is more suitable for the synthesis of MCM-41. Therefore, this optimum condition was based on the synthesis of metal supported MCM-41. Metal supported MCM-41 materials (metal: aluminum, cobalt iron,) with different metal/Si molar ratios (metal/Si: 0.05, 0.1 and 0.2) were synthesized at optimum conditions.

3.2. Characterization of Al-MCM-41

The XRD patterns of Al-MCM-41 with different Al/Si molar ratios were given in Figure 4 (according to increasing ratios, samples were named 1, 2, and 3, respectively). In all figures, the prominent peak indicating incorporation of Al^{3+} framework of siliceous MCM-41 was observed. The amorphous silica structure peak was observed approximately in the range of 2θ: 20-30° angles. The intensity of this peak increased as the Al / Si ratio increases.

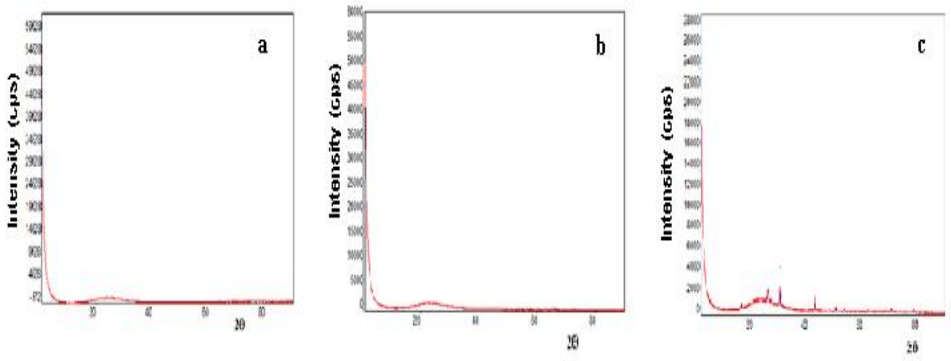

FIGURE 4. X-ray powder diffraction patterns of sample (a) Al-1, (b) Al-2, (c) Al-3.

The SEM images of Al-MCM-41 with different molar ratios were shown in Figure 5. All the supporting materials appeared to be a well-defined arrangement in particle morphology with uniform diameters of smaller than 30 nm.

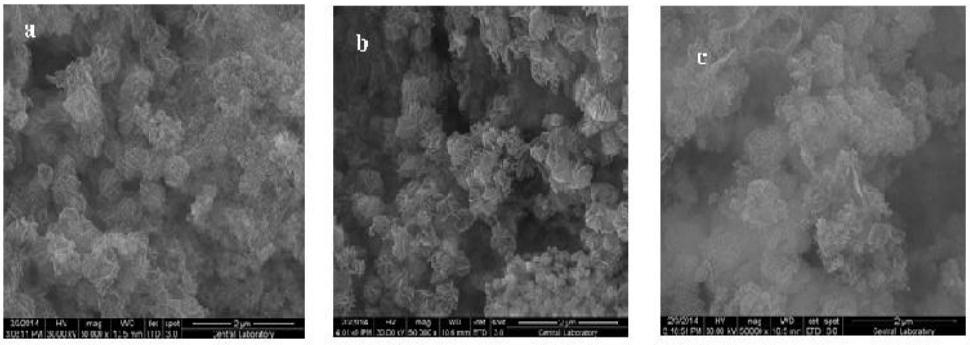

FIGURE 5. Scanning electron micrographs for sample (a) Al-1, (b) Al-2, (c) Al-3.

The elemental composition of synthesized metal supported MCM-41 materials was identified with the EDS method. Al/Si molar ratios in bulk obtained for Al-MCM-41 material calculated from their EDS results were summarized together with BET analyses in Table 5. The Al/Si molar ratios in the synthesized Al-MCM-41 were much higher than the Al/Si molar ratios in the synthesis mixture. These results showed that Al was successfully supported into the MCM-41 structure. Higher Al/Si ratios in the concrete matrix than the corresponding values in the solution indicated the loss of some of the Si during the synthesis materials' washing procedure. As seen in Table 5, the BET surface area of Al-MCM-41 materials was lower than the surface area of pure MCM-41, which indicated that some of the smaller pores present in the

structure of MCM-41 were plugged by large Al clusters. A decreasing trend of BET surface area was observed with an increase in Al/Si ratio.

TABLE 5. EDS analysis and BET surface area value for Al, Co, and Fe supported MCM-41 samples with different metal /Si molar ratios.

Sample	**metal/Si atomic ratio (In the solution)**	**metal/Si atomic ratio (In the bulk)**	**BET surface area (m^2/g)**
Al-MCM-41	0.2	0.26	369
Al-MCM-41	0.1	0.17	502
Al-MCM-41	0.05	0.09	776
Co-MCM-41	0.2	0.33	337
Co-MCM-41	0.1	0.28	318
Co-MCM-41	0.05	0.09	301
Fe-MCM-41	0.2	0.24	393
Fe-MCM-41	0.1	0.14	447
Fe-MCM-41	0.05	0.06	462

3.3. Characterization of Co-MCM-41

Figure 6 illustrated the XRD patterns of the Co-MCM-41 material with Co/Si molar ratios of 0.05, 0.1, and 0.2 (were named as Co-1, Co-2, and Co-3, respectively). As seen in the figure, the characteristic peak of MCM-41 was retained in all the synthesized Co-MCM-41 samples. These show that the cobalt introduction did not destroy the MCM-41 structure, and the samples preserve the crystalline properties.

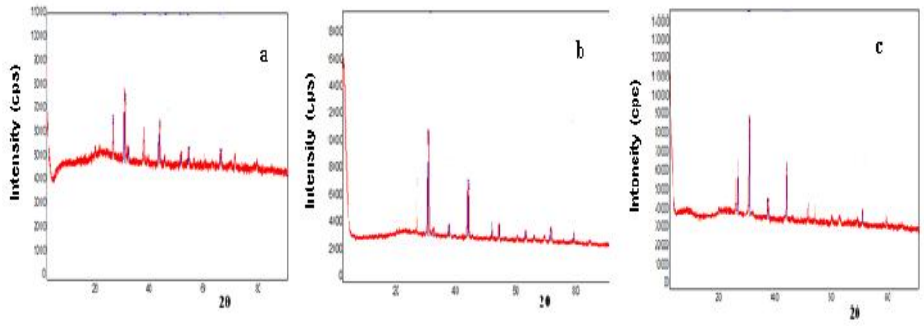

FIGURE 6. X-ray powder diffraction patterns of sample (a) Co-1, (b) Co-2, (c) Co-3.

The SEM images of the synthesized Co-MCM-41 catalyst were given in Figure 7. As seen in this figure, the particle diameter of the Co-MCM-41 samples was fallen below 10 nm. Also, small particles, agglomeration, and rod structure were observed on Co-MCM-41 samples.

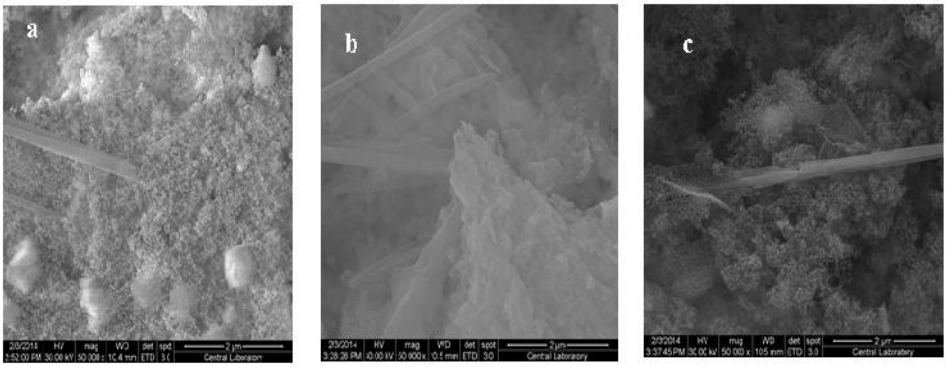

FIGURE 7. Scanning electron micrographs for sample (a) Co-1, (b) Co-2, (c) Co-3.

The EDS analysis results and BET values of Co-1, Co-2, and Co-3 were summarized in Table 5. These results indicated that impregnation of Co in the structure of MCM-41 was successfully achieved. As mentioned earlier, higher Co/Si ratios in the concrete matrix than the corresponding values in the solution indicate the loss of some of the Si during the washing procedure. BET surface areas of MCM-41 samples were more significant than that of Co-MCM-41 (see Table 5). This result indicates that Co was deposited in the pores of MCM-41. Higher content of cobalt was correlated with a little increase in the surface area.

3.4.Characterization of Fe-MCM-41

The XRD pattern of the synthesized Fe-MCM-41 with different molar ratios was given in Figure 8. It is seen the characteristic peaks of the MCM-41. The peaks of the Fe_2O_3 phase formed by iron's addition were observed in the range of 30-40 °angles. Also, the increasing Fe/Si ratio and iron addition could not settle into the crystal lattice and formed the Fe_2O_3 phase in the materials' outer surface.

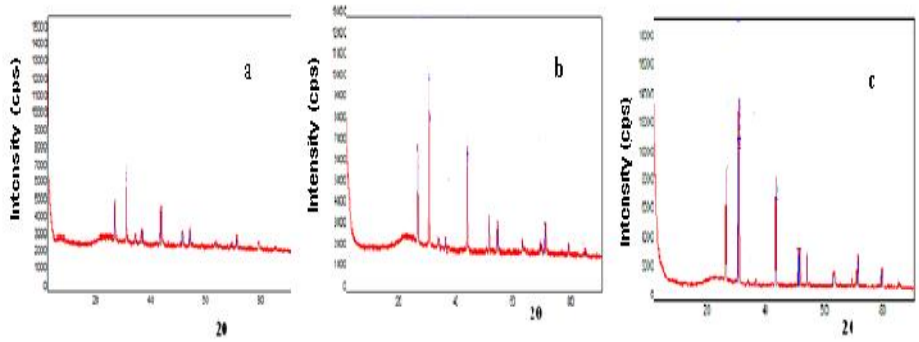

FIGURE 8. X-ray powder diffraction patterns of sample (a) Fe-1, (b) Fe-2, (c) Fe-3.

Figure 9 show SEM images of Fe-MCM-41 samples. SEM micrographs indicated that Fe-MCM-41 materials have a morphology of agglomerates. The average particle size of the sample was estimated to be smaller than 10 nm.

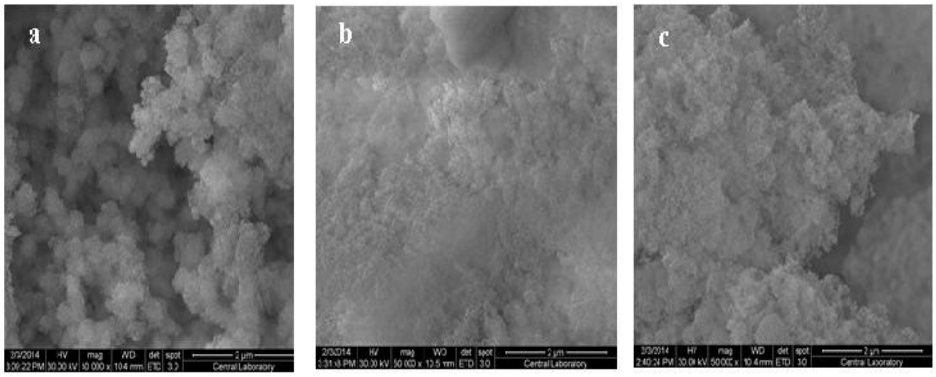

FIGURE 9. Scanning electron micrographs for sample (a) Fe-1, (b) Fe-2, (c) Fe-3.

The EDS analysis results and BET values of Fe-MCM-41 materials with different Fe/Si ratios were summarized in Table 5. It is seen that for all the synthesized samples, the Fe/Si molar ratios in the product were higher than the corresponding ratio in the solution. These results showed that the impregnation of Fe in the structure of MCM-41 was successfully achieved. As seen in Table 5, a decreasing trend was observed in the BET surface area, increasing the Fe/Si ratio. The reason was that the pores partially closed by collapsing silicate groups with the addition of a large amount of iron in the structure, and the inner walls of the pore, which are known to contribute surface area, were blocked.

4. Conclusion

MCM-41 material, which has a high surface area and pore size distribution, was synthesized using the hydrothermal and sonochemical methods using suitable synthesis conditions. Different characterization methods investigated the physical properties of synthesized materials. The analysis results determined that the pores in the structure of the MCM-41 sample show a uniform distribution on the hexagonal shape similar to the literature. When the synthesis methods are compared, it was observed that the mixture formed by using ultrasound was homogeneous and obtained in a shorter time. This result showed that the sonochemical method was more useful in the synthesis of MCM-41.

The effects of silica sources on the synthesis of MCM-41 material were investigated, and the results showed that silica sources influence the surface area, pore-volume, and morphology of the material. Using sodium silicate as a silica source, the MCM-41 crystal structure was found better than the others and have a higher specific surface area and pore volume.

Metal-MCM-41 materials were obtained by incorporating different metal / Si molar ratios (0.05, 0.1, and 0.2) of the metal source (Al, Co, Fe) on the MCM-41 structure. To determine the structural properties of synthesized metal-MCM-41 materials, different characterization methods were used. The XRD results showed that impregnation of metal sources in the structure of MCM-41 does not disrupt the characteristic structure of MCM-41, and XRD peak intensities of MCM-41 samples were found to be higher than the peak intensity of metal-MCM-41 samples. Considering the BET results of metal-MCM-41 samples, the supported metal source in the structure was concluded by the effect on the wall thickness and mesopore size. From the EDS analysis results of metal-MCM-41 samples, the Metal/Si molar ratios in the synthesized material were consistent with the solution's corresponding ratio. Better incorporation of metal sources on the structure was thought to result from prepared the metal solution and synthesis mixture during the synthesis process.

As a result, the sonochemical synthesis of MCM-41 and metal-supported MCM-41 with the aid of a silica source, namely sodium silicate, was quite successful in terms of controlling and determining the high surface areas and pore volumes. Due to high surface area and large pore volume, synthesized mesoporous materials may be a promising catalyst for the pyrolysis of different biomasses. The catalytic properties of these catalysts should also be investigated.

Acknowledgement. This work is financially supported by Ankara University, BAP, under project number "12B4240007". The authors thank Ankara University BAP for their support.

REFERENCES

[1] Jabariyan, S., Zanjanchi, M. A., A simple and fast sonication procedure to remove surfactant templates from mesoporous MCM-41, *Ultrasonics Sonochemistry*, 19 (2012), 1087-1093.

[2] Øye, G., Glomm, W. R., Vrålstad, T., Volden, S., Magnusson, H., Stöcker, M., Sjöblom, J., Synthesis, functionalization and characterization of mesoporous materials and sol-gel glasses for application in catalysis, adsorption and photonics, *Advances in Colloid and Interface Science*, 123 (2006), 17-32.

[3] Jentys, A., Pham, N. H., Vinek, H., Englisch, M., Lercher, J. A., Synthesis and characterization of mesoporic materials containing highly dispersed cobalt, *Microporous Materials*, 68 (1996), 13-17.

[4] Beck, J. S., Vartuli, J. C., Roth, W. J., Leonowicz, M. E., Kresge, C. T., Schmitt, K. D., Chu, C. T. W., Olson, D. H., Sheppard, E. W., McCullen, S. B., Higgins, J. B., Schlenker, J. L., A new family of mesoporous molecular sieves prepared with liquid crystal templates, *Journal of the American Chemical Society*, 114 (1992),10834-10843.

[5] Nejabat, G. R., Nekoomanesh, M., Arabi, H., Emami, M., Aghaei-Nieat, M., Preparation of polyethylene nano-fibres using rod-like MCM-41/$TiCl_4$/$MgCl_2$/THF Bi-supported Ziegler-natta catalytic system, *Iranian Polymer Journal*, 19 (2010), 79-87.

[6] Huang, R. H., Liu, J., Li, L. S., Zhang, Q. Y., Zeng, L. X., Lu, P., Fe/MCM-41 as a promising heterogeneous catalyst for ozonation of p-chlorobenzoic acid in aqueous solution, *Chinese Chemical Letters*, 22 (2011), 683-686.

[7] Gucbilmez, Y., Dogu, T., Balci, S., Vanadium incorporated high surface area MCM-41 catalysts, *Catalysis Today*, 100 (2005), 473-477.

[8] Gaydhankar, T. R., Samuel, V., Jha, R. K., Kumar, R., Joshi, P. N., Room temperature synthesis of Si-MCM-41 using polymeric version of ethyl silicate as a source of silica, *Materials Research Bulletin*, 42 (2007),1473-1484.

[9] Voegtlin, A. C., Matijasic, A., Patarin, J., Sauerland, C., Grillet, Y., Huve, L., Room-temperature synthesis of silicate mesoporous MCM-41-type materials: influence of synthesis pH on the porosity of the materials obtained, *Microporous Materials*, 10 (1997), 137-147.

[10] Kruk, M., Jaronice, M., Sayari, A., Structure and surface properties of siliceous and titanium-modified HMS molecular sieves, *Microporous and Mesoporous Materials*, 35 (2000), 545-553.

[11] Aquino, J. M. F. B., Souza, C. D. R., Aroujo, A. S., Synthesis and characterization of sulfate-supported MCM-41 material, *International Journal of Inorganic Materials*, 3(2001), 467-470.

[12] Tai, X. M., Wang, H. X., Shi, X. Q., A novel method for the synthesis of mesoporous molecular sieve MCM-41, *Chinese Chemical Letter*, 16 (2005), 843-845.

[13] Zanjanchi, M. A., Asgari, S., Incorporotion of aluminum into the framework of

mesoporous MCM-41: the contribution of diffuse reflectance spectroscopy, *Solid State Ionics*, 171 (2004), 277-282.

[14] Melo, R. A. A, Giottoa, M. V., Rochab, J., Ernesto, A. González, U., MCM-41 Ordered mesoporous molecular sieve synthesis and characterization, *Materials Research*, 2 (1999), 173-179.

[15] Suslick, K. S., Interparticle collisions driven by ultrasound, *Science*, 247 (1990), 1437-1445.

[16] Horòáèek, M., Hudec, P., Smiešková, A., Syntesis and characterization of mesoporous molecular sieves, *Chemical Papers*, 63 (2009), 689-697.

[17] Sun, Z., Wang, L., Liu, P., Sun, B., Jiang, D., Xiao, F., Synthesis and catalytic activity of Cu-incorporated MCM-41 with spheres-within-a-sphere hollow structure, *Chinese Journal of Chemistry*, 24(2006), 1653-1656.

[18] Eimer, G. A., Pierella, L. B., Monti, G. A., Anunziata, O. A., Synthesis and characterization of Al-MCM-41 and Al-MCM-48 mesoporous materials, *Catalysis Letters*, 78 (2002), 65-75.

[19] Huang, R. H., Liu, J, Li, L. S., Zhang, Q. Y., Zeng, L. X., Lu, P., Fe/MCM-41 as a promising heterogeneous catalyst for ozonation of p-chlorobenzoic acid in aqueous solution, *Chinese Chemical Letters*, 22 (2011), 683-686.

[20] Lemus, I. A., Gomez, Y. V., Elguézabal, A. A., Contreras, L. A., Metal nanoparticles supported on Al-MCM-41 via in situ aqueous synthesis, *Journal of Nanomaterials*, 2010 (2010), 1-8.

[21] Gedikli, Ü., Mısırlıoğlu, Z., Bozkurt P. A., Canel, M., Synthesis of MCM-41 by hydrothermal and sonochemical methods and characterization, *Journal of the Turkish Chemical Society, Section A: Chemistry*, 2 (2015), 54-58.

[22] Li, Q., Brown, S. E., Broadbelt, L. J., Zheng, J. G., Wu, N. Q., Synthesis and characterization of MCM-41 supported Ba_2SiO_4 base catalyst, *Microporous and Mesoporous Materials*, 59 (2003), 105-111.

[23] Lensveld, D. J., Mesu, J. G., Dillen, A. J., Jong, K. P., Synthesis and characterization of MCM-41 supported nickel oxide catalyst, *Microporous and Mesoporous Materials*, 44 (2001), 401-407.

[24] Hui, K. S., Chao, C. Y. H., Synthesis of MCM-41 from coal fly ash by a green approach: Influence of synthesis pH, *Journal of Hazardous Materials B*, 137 (2006), 1135-1148.

[25] Fu, L., Zhang, H., Preparation, characterization and luminescent properties of MCM-41 type materials impregnated with rare earth complex, *Journal of Materials Science and Technology*, 17 (2001), 293-298.

[26] Somani, R. S., Textural and structural properties of mesoporous silica synthesized under refluxing conditions, *Journal of Porous Materials*, 12 (2005), 87-94.

[27] Laha, S. C., Mukherjee, P., Kumar, R., Synthesis and characterization of surface-modified and organic-functionalized MCM-41 type ordered mesoporous materials, *Bulletin of Materials Science*, 22 (1999), 623-626.

[28] Liu, D., Quek, X. Y., Cheo, W. N. E., Lau, R., Borgna, A., Yang, Y., MCM-41 supported nickel-based bimetallic catalysts with superior stability during carbon dioxide reforming of methane: effect of strong metal-support interaction, *Journal of Catalysis*, 266 (2009), 380-390.

[29] Blin, J. L., Otjacques, C., Herrier, G, Su, B. L., Kinetic study of MCM-41 synthesis, International Journal of Inorganic Materials, 3 (2001) 75-86.

[30] Yu, J., Shi, J. L., Wang, L. Z., Ruan, M. L., Yan, D. S., Preparation of high thermal stability MCM-41 in the low surfactant/silicon molar ration synthesis systems, *Materials Letters*, 48 (2001), 112-116.